

# A thermodynamic and crystallographic study of complexes of the highly preorganized ligand 8-hydroxyquinoline-2-carboxylic acid

F. Crisp McDonald<sup>a</sup>, Rachel C. Applefield<sup>a</sup>, Christopher J. Halkides<sup>a</sup>,  
Joseph H. Reibenspies<sup>b</sup>, Robert D. Hancock<sup>a,\*</sup>

<sup>a</sup> Department of Chemistry and Biochemistry, University of North Carolina at Wilmington, Wilmington, NC 28403, USA

<sup>b</sup> Department of Chemistry, Texas A&M University, College Station, TX 77843, USA

Received 13 April 2007; received in revised form 27 September 2007; accepted 7 October 2007

Available online 12 October 2007

## Abstract

The metal ion complexing properties of the ligand HQC (8-hydroxyquinoline-2-carboxylic acid) are reported. The structures of  $[\text{Zn}(\text{HQCH})_2] \cdot 3\text{H}_2\text{O}$  (**1**) and  $[\text{Cd}(\text{HQCH})_2] \cdot 3\text{H}_2\text{O}$  (**2**) were determined (HQCH = HQC with phenol protonated). Both **1** and **2** are triclinic, space group  $P\bar{1}$ , with  $Z = 2$ . For **1**  $a = 7.152(3)$ ,  $b = 9.227(4)$ ,  $c = 15.629(7)$  Å,  $\alpha = 103.978(7)^\circ$ ,  $\beta = 94.896(7)^\circ$ ,  $\gamma = 108.033(8)^\circ$ ,  $R = 0.0499$ . For **2**  $a = 7.0897(5)$ ,  $b = 9.1674(7)$ ,  $c = 16.0672(11)$  Å,  $\alpha = 105.0240(10)^\circ$ ,  $\beta = 93.9910(10)^\circ$ ,  $\gamma = 107.1270(10)^\circ$ ,  $R = 0.0330$ . In **1** the Zn has a distorted octahedral coordination geometry, with Zn–N of 2.00 and 2.15 Å, and Zn–O to the protonated phenolic oxygens of 2.431 and 2.220 Å. The structure of **2** is similar, with Cd–N bonds of 2.220 and 2.228 Å, with Cd–O bonds to the protonated phenolate oxygens of 2.334 and 2.463 Å. The structures of **1** and **2**, and isomorphous Ni(II) and Co(II) HQC complexes reported in the literature, show very interesting short ( $<2.5$  Å) O–O distances in H-bonds involving the protons on the coordinated phenolates and lattice water molecules. These are discussed in relation to the possible role of short low-energy H-bonds in alcohol dehydrogenase in mediating the transfer of the hydroxyl proton of the alcohol to an adjacent serine oxygen.

The formation constants for HQC are determined by UV–Visible spectroscopy at 25 °C in 0.1 M NaClO<sub>4</sub> with Mg(II), Ca(II), Sr(II), Ba(II), La(III), Gd(III), Zn(II), Cd(II), Ni(II), Cu(II), and Pb(II). These show greatest stabilization with metal ions with an ionic radius above 1.0 Å. This is as would be expected from the fact that HQC forms two five-membered chelate rings on complex-formation, which favors larger metal ions. The ligand design concept of using rigid aromatic backbones in ligands to achieve high levels of preorganization, and hence the high log  $K$  values (for a tridentate ligand) and strong metal ion selectivities observed for HQC, is discussed.

© 2007 Elsevier B.V. All rights reserved.

**Keywords:** X-ray crystal structure; Formation constants; Ligand preorganization; Metal ion recognition; Cadmium; Zinc; Lead; Copper; Nickel; Calcium; Magnesium; Strontium; Barium; Lanthanum; Gadolinium; 8-Hydroxyquinoline-2-carboxylic acid; 8-Hydroxyquinoline; Ligand design

## 1. Introduction

The concept of preorganization was first introduced by Cram [1]. A ligand is more highly preorganized the more it is as a free ligand constrained to be in the conformation required to complex a target metal ion [1,2]. Areas where ligand design, and thus preorganization, is important, range from biomedical applications [3] to recovery of metal

ions from radioactive wastes [4]. Classical examples of pre-organized ligands are macrocycles, such as crown ethers [5], N-donor macrocycles, including more recent reinforced examples [6], and cryptands [7]. Much less well recognized are non-macrocyclic ligands that are highly preorganized, primarily those based on cyclohexylene bridges [8–11], where the rigid cyclohexylene bridge leads to complexes of enhanced thermodynamic stability as compared to analogs with ethylene bridges. Ligands where the donor atoms are part of, or attached to, polynuclear aromatics, such as 1,10-phen or oxine (see Fig. 1 for key to ligand

\* Corresponding author. Tel.: +1 910 962 3025; fax: +1 910 962 3013.

E-mail address: [hancockr@uncw.edu](mailto:hancockr@uncw.edu) (R.D. Hancock).

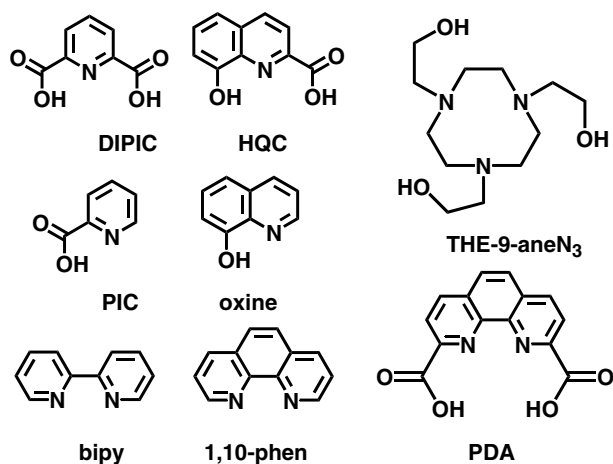


Fig. 1. Ligands discussed in this paper.

abbreviations) are also highly preorganized because of the rigidity of the aromatic systems [2], although this is not generally recognized to be the case. The effect of such preorganization can be seen in that  $\log K_1$  (the formation constant) for complexes [12] of 1,10-phen is somewhat higher than for the less preorganized analogue, bipy. Thus,  $\log K_1$  for 1,10-phen complexes is generally about 1.4 log units higher [2,12] than for the analogous bipy complexes. This modest stabilization arises because in 1,10-phen complexes only a single chelate ring is being preorganized. We report here a study of the complexes of HQC, where two highly preorganized chelate rings can be formed. Of particular importance is that both of these chelate rings will be five-membered, which should favor larger metal ions [2] with an ionic radius [13] of about 1.0 Å. The protonation constants for HQC, and its  $\log K_1$  values with a range of metal ions, are reported. There has been a report [14] of a potentiometric study of HQC complexes, but this was carried out in 50% dioxan, which does not allow for direct comparison of the  $\log K_1$  values measured with those determined in aqueous solution for other similar ligands.

The crystal structures of complexes with Zn(II) and Cd(II) with HQC, which complement the known structures of the Cu(II), Ni(II) and Co(II) complexes [15–17], are reported. The structures of the complexes of the very rigid HQC ligand reported here appear to show a sequence of transfers of a proton from a coordinated phenolate group to an adjacent water molecule as the metal ion changes along the series Ni(II) to Zn(II) and then to Cd(II). It appears that the rigidity of the HQC ligand controls how closely the metal ion can approach the protonated phenol group, and thus controls the strength of interaction of the metal ion with the phenolate oxygen donor. The structures of  $[M(HQCH)_2] \cdot 3H_2O$  complexes show very short H-bonds between the coordinated phenolic oxygens and adjacent water molecules. Such low barrier H-bonds, with O–O separations of about 2.45–2.50 Å instead of the more usual separations of 2.6–2.9 Å for H-bonds (hydrogen bonds) involving two O-atoms, are thought to be of impor-

tance in catalysis in biology [18,19], and possibly also in ADH (alcohol dehydrogenase) [20].

## 2. Experimental

### 2.1. Materials

The ligand 8-hydroxyquinoline-2-carboxylic acid (>98% purity) was obtained from Fluka, and metal perchlorates used were obtained in at least 99% purity from VWR. These materials were used as received. All solutions were made up in deionized water (Milli-Q, Waters Corp.) of  $>18 \text{ M}\Omega \text{ cm}^{-1}$  resistivity.

### 2.2. Synthesis of $[Zn(HQCH)_2] \cdot 3H_2O$ (1) and $[Cd(HQCH)_2] \cdot 3H_2O$ (2)

HQC (~0.1 g) was dissolved in 20 mL *n*-butanol, and the metal perchlorate (1 equiv) was dissolved in ~20 mL of deionized water. The metal perchlorate solution was then added drop wise carefully down the side of the 50 mL beaker containing the ligand solution so as not to disturb the solvent/solvent interface. The beaker was covered with Parafilm, in which small holes were made to allow for slow evaporation. After one month the colorless crystals that had grown at the interface were collected. Elemental *Anal.* Calc. for **1**,  $C_{20}H_{18}N_2O_9Zn$ , C, 48.45; H, 3.66; N, 5.65. Found: C, 49.10; H, 3.78; N, 5.32%. *Anal.* Calc. for **2**,  $C_{20}H_{18}N_2O_9Cd$ , C, 44.26; H, 3.34; N, 5.16. Found: C, 44.46; H, 3.31; N, 5.31%.

### 2.3. Molecular structure determination

A Bruker SMART 1K diffractometer using the omega scan mode was employed for crystal screening, unit cell determination, and data collection at 110(2) K. The structures were solved by direct methods and refined to convergence [21]. Absorption corrections were made using the SADABS program [22]. All hydrogens were located in difference Fourier maps (including those at ideal positions). Some details of the structure determinations are given in Table 1, and crystal coordinates and details of the structure determinations of **1** and **2** have been deposited with the CSD (Cambridge Structural Database) [23]. A selection of bond lengths and angles for **1** and **2** is given in Tables 2 and 3, and the structures of **1** and **2** are shown in Figs. 2 and 3.

### 2.4. Formation constant studies

The metal ion complexing properties of HQC can be studied by recording the electronic spectra of solutions of  $2 \times 10^{-5} \text{ M}$  ligand in the range 350–190 nm as a function of pH, in the presence of varying concentrations of metal ions. The approach is similar to that used by Choppin et al. [24] to study the complexes of Nd(III) and Th(IV) with ligands such as oxine and 1,10-phen. The studies were

Table 1

Crystallographic data for  $[\text{Zn}(\text{HQCH})_2] \cdot 3\text{H}_2\text{O}$  (**1**) and  $[\text{Cd}(\text{HQCH})_2] \cdot 3\text{H}_2\text{O}$  (**2**)

	<b>1</b>	<b>2</b>
Empirical formula	$\text{C}_{20}\text{H}_{18}\text{N}_2\text{O}_9\text{Zn}$	$\text{C}_{20}\text{H}_{18}\text{N}_2\text{O}_9\text{Cd}$
Formula weight	495.73	542.76
<i>T</i> (K)	110(2)	110(2)
Crystal system	triclinic	triclinic
Space group	<i>P</i> $\bar{1}$	<i>P</i> $\bar{1}$
<i>a</i> (Å)	7.152(3)	7.0897(5)
<i>b</i> (Å)	9.227(4)	9.1674(7)
<i>c</i> (Å)	15.629(7)	16.0672(11)
<i>V</i> (Å <sup>3</sup> )	937.3(7)	951.73(12)
$\alpha$ (°)	103.978(7)	105.0240(10)
$\beta$ (°)	94.896(7)	93.9910(10)
$\gamma$ (°)	108.033(8)	107.1270(10)
<i>Z</i>	2	2
$\mu$ (mm <sup>−1</sup> )	1.373	1.894
Reflections collected	11 036	10 258
Independent reflections ( <i>R</i> <sub>int</sub> )	3214 (0.0581)	3098 (0.0206)
Final <i>R</i> indices [ <i>I</i> > 2σ( <i>I</i> )]	<i>R</i> <sub>1</sub> = 0.0499, <i>wR</i> <sub>2</sub> = 0.0822	<i>R</i> <sub>1</sub> = 0.0330, <i>wR</i> <sub>2</sub> = 0.0798
<i>R</i> indices (all data)	<i>R</i> <sub>1</sub> = 0.0673, <i>wR</i> <sub>2</sub> = 0.0873	<i>R</i> <sub>1</sub> = 0.0355, <i>wR</i> <sub>2</sub> = 0.0822

carried out in 0.1 M NaClO<sub>4</sub> at 25.0 ± 0.1 °C. UV–Visible spectra were recorded using a Varian 300 Cary 1E UV–Visible Spectrophotometer controlled by Cary Win UV Scan Application version 02.00(5) software. A VWR symphony™ SR60IC pH meter with a VWR symphony™ gel epoxy semi-micro combination pH electrode was used for all pH readings. The pH meter was calibrated prior to every titration, and standardized using pH 4.00, 7.00, and 10.00 (±0.01) buffers (Fisher). The cell containing 50 ml of ligand/metal solution was placed in a bath thermostated to 25.0 °C, and a peristaltic pump was used to circulate the solution through a flow cell situated in the spectrophotometer. The pH was altered in the range 2–12 by additions of small amounts of HClO<sub>4</sub> or NaOH as required using a micropipette. After each adjustment of pH, the system was allowed to mix by operation of the peristaltic pump for 15 min prior to recording the spectrum.

Table 2

Selection of bond lengths (Å) and angles (°) for **1** ( $[\text{Zn}(\text{HQCH})_2] \cdot 3\text{H}_2\text{O}$ )

<b>Bond lengths</b>					
Zn(1)–N(1)	2.003(3)	Zn(1)–N(2)	2.015(3)	Zn(1)–O(4)	2.082(3)
Zn(1)–O(3)	2.220(4)	Zn(1)–O(1)	2.225(3)	Zn(1)–O(6)	2.431(3)
O(3)–H(1wB)	1.20(7)	O(2w)–H(1wB)	1.29(7)		
<b>Bond angles</b>					
N(1)–Zn(1)–N(2)	164.44(12)	N(1)–Zn(1)–O(4)	115.72(10)		
N(2)–Zn(1)–O(4)	79.74(11)	N(1)–Zn(1)–O(3)	76.43(11)		
N(2)–Zn(1)–O(3)	106.20(11)	O(3)–Zn(1)–O(4)	91.66(10)		
N(1)–Zn(1)–O(5)	75.60(10)	N(2)–Zn(1)–O(1)	101.25(10)		
O(1)–Zn(1)–O(4)	98.74(10)	O(3)–Zn(1)–O(1)	151.97(9)		
N(1)–Zn(1)–O(6)	93.61(10)	N(2)–Zn(1)–O(4)	71.06(11)		
O(4)–Zn(1)–O(6)	150.60(9)	O(3)–Zn(1)–O(6)	93.44(10)		
O(6)–Zn(1)–O(1)	90.13(10)	Zn(1)–O(3)–H(1wB)	116(3)		
C(9)–O(3)–H(1wB)	115(3)	O(3)–H(1wB)–O(2w)	164(5)		

Table 3

Selection of bond lengths (Å) and angles (°) for **2** ( $[\text{Cd}(\text{HQCH})_2] \cdot 3\text{H}_2\text{O}$ )

<b>Bond lengths</b>					
Cd(1)–N(2)	2.228(3)	Cd(1)–N(1)	2.200(3)	Cd(1)–O(3)	2.334(2)
Cd(1)–O(4)	2.463(2)	Cd(1)–O(5)	2.299(2)	Cd(1)–O(1)	2.382(3)
<b>Bond angles</b>					
N(2)–Cd(1)–N(1)	169.00(10)	N(2)–Cd(1)–O(3)	111.71(9)		
N(1)–Cd(1)–O(3)	72.47(9)	N(2)–Cd(1)–O(4)	68.82(9)		
N(1)–Cd(1)–O(4)	100.83(8)	O(3)–Cd(1)–O(4)	97.59(8)		
N(2)–Cd(1)–O(5)	72.60(9)	N(1)–Cd(1)–O(5)	117.82(8)		
O(3)–Cd(1)–O(5)	94.29(8)	O(4)–Cd(1)–O(5)	141.35(8)		
N(2)–Cd(1)–O(1)	104.86(9)	N(1)–Cd(1)–O(1)	70.02(9)		
O(3)–Cd(1)–O(1)	143.26(8)	O(4)–Cd(1)–O(1)	92.15(8)		
O(5)–Cd(1)–O(1)	99.90(8)	C(1)–O(1)–Cd(1)	115.0(2)		
C(9)–O(3)–H(1wB)	114(5)	Cd(1)–O(3)–H(1wB)	119(5)		

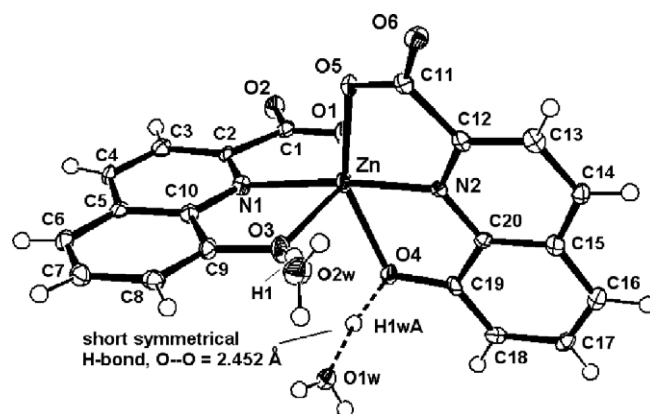


Fig. 2. Structure of the  $[\text{Zn}(\text{HQCH})_2]$  complex (**1**) showing the numbering scheme of the donor atoms coordinated to the Zn. Also shown is a water molecule (O(8)) that forms a short symmetrical H-bond to the O(4) phenolate oxygen of one HQCH ligand, and to a carboxylate oxygen (not shown) of a neighboring  $[\text{Zn}(\text{HQCH})_2]$  individual. Drawing made using ORTEP [28].

Study of the ligand alone yields two inflections in the curves of absorbance versus pH at 10 different wavelengths, which are interpreted as two protonation constants,  $\text{p}K_{\text{a}}(1)$  and  $\text{p}K_{\text{a}}(2)$ . The spectra of  $2 \times 10^{-5}$  M HQC in 0.1 M

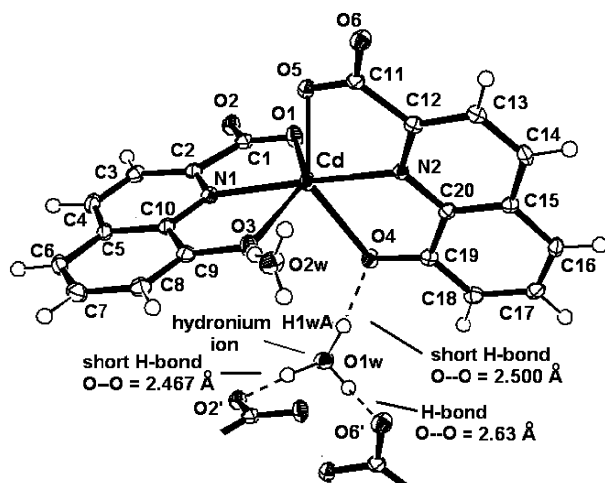


Fig. 3. Structure of the  $[\text{Cd}(\text{HQCH})_2]$  complex (2) showing the atom numbering scheme. Also shown is a hydronium ion that forms short H-bonds to the O(3) phenolate oxygen of one HQC ligand, and to a carboxylate oxygen (O(6)) of a neighboring  $[\text{Cd}(\text{HQCH})_2]$  individual. Drawing made using ORTEP [28].

$\text{NaClO}_4$  with no metal added, as a function of pH, are seen in Fig. 4a. In Fig. 4b, the variation of the absorbance of HQC at 250 and 265 nm as a function of pH is shown. The solid lines in Fig. 4b are for a theoretical curve generated from protonation constants of  $\text{p}K_{\text{a}}(1) = 9.98$  and  $\text{p}K_{\text{a}}(2) = 3.94$ . The curve was fitted using the SOLVER module of EXCEL [25], which was used here for all spectral data fitting. In the presence of metal ions, several protonation equilibria are indicated by the variation of the spectra of HQC solutions with pH. Two at lower pH are interpreted as protonation of HQC, shifted to lower pH because of the competition between protons and metal ion for binding sites on the ligand. For less acidic metal ions such as  $\text{Mg}(\text{II})$  or  $\text{Ca}(\text{II})$ , these are the only protonation equilibria

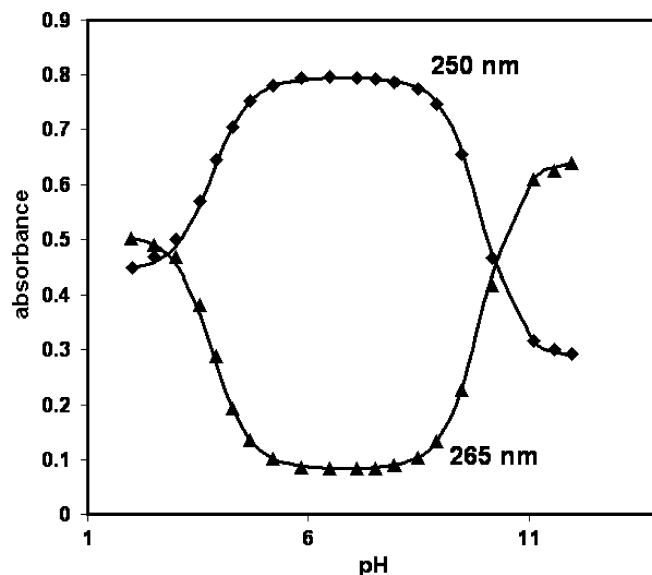


Fig. 4b. Variation of absorbance at 250 (◆) and 265 (▲) nm for  $2.00 \times 10^{-5}$  M HQC in 0.1 M  $\text{NaClO}_4$  as a function of pH. Solid lines are theoretical curves fitted with  $\text{p}K_{\text{a}}(1) = 9.98$  and  $\text{p}K_{\text{a}}(2) = 3.84$  for HQC.

observed in the pH range 2–12. In Fig. 5a is shown the set of spectra of  $\text{Gd}(\text{III})/\text{HQC}$  solutions in the pH range 2–12 is shown, and in Fig. 5b the variation of absorbance for these spectra as a function of pH at five different wavelengths is shown. Apparent protonation constants can be calculated in the presence of these metal ions, which are the midpoints ( $\text{pH}_{50}$ ) in the inflections of absorbance versus pH. The formation constants can be calculated from

$$\text{Log}K_1 = (\text{p}K_{\text{a}}(1) + \text{p}K_{\text{a}}(2))_{\text{free ligand}} - (\text{p}K_{\text{a}}(1) + \text{p}K_{\text{a}}(2))_{\text{apparent}} + [\text{M}^{n+}] \quad (1)$$

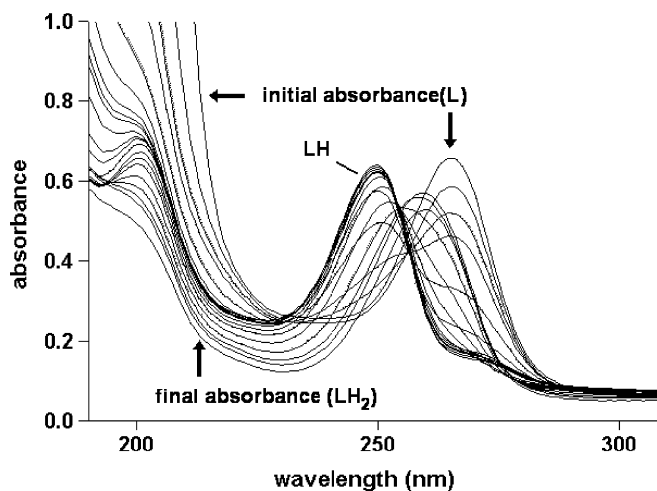


Fig. 4a. Absorption spectra of  $2.00 \times 10^{-5}$  M HQC ligand in 0.1 M  $\text{NaClO}_4$  at 25 °C as a function of pH. The initial absorbance is at pH 11.97 and the final absorbance is at pH 1.49. The spectra where the different protonated forms (LH and  $\text{LH}_2$ ) of HQC (L) are dominant are indicated.

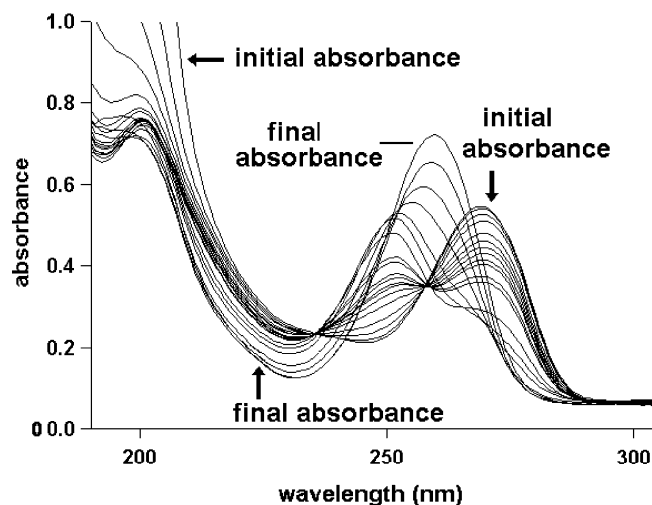


Fig. 5a. Absorption spectra of  $2 \times 10^{-5}$  M HQC ligand plus  $2 \times 10^{-5}$  M  $\text{Gd}^{3+}$  in 0.1 M  $\text{NaClO}_4$  at 25 °C as a function of pH. The initial absorbance is at pH 11.05 and the final absorbance is at pH 2.04.

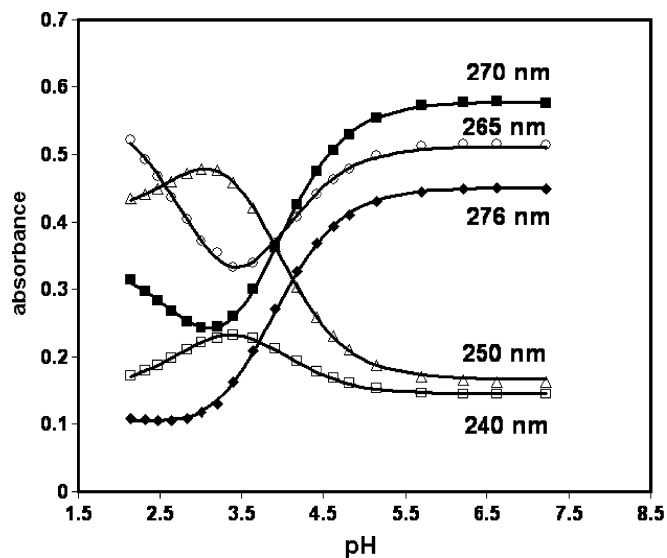
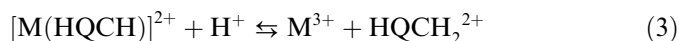


Fig. 5b. Variation of absorbance with pH at five different wavelengths for a solution containing  $2 \times 10^{-5}$  M HQC and  $2 \times 10^{-5}$  M  $\text{Gd}^{3+}$  in 0.1 M  $\text{NaClO}_4$ . The solid lines are theoretical curves calculated from  $\text{pH}_{50}$  values of 3.87 and 2.92, and appropriate molar absorptivities for the  $\text{GdL}$ ,  $\text{GdLH}$  and  $\text{LH}$  species in solution at each wavelength.

The protonation equilibrium at higher pH for  $\text{Gd(III)}$  depicted in Fig. 5a, with a mid-point in its inflection at pH 3.87, is interpreted as the equilibrium



The protonation equilibrium at lower pH is interpreted as the equilibrium



One can be reasonably sure of this interpretation, because for all metal ions, at pH values below the low pH protonation equilibrium in Eq. (3), the electronic spectrum of the solution is identical to that of the ligand on its own at the same pH values. One can also be reasonably sure that the metal ion is still complexed by the ligand as suggested in Eq. (2), because the spectra below the pH of this protonation equilibrium involving the phenolate oxygen are not the same as for the free ligand, until the pH of Eq. (3) is reached. The crystal structures reported here for the  $\text{Zn(II)}$  and  $\text{Cd(II)}$  complexes of HQC also support this interpretation in that they show protonated phenolate oxygens coordinated to the metal ions. Where experiments were carried out with equimolar concentrations of  $\text{M}^{n+}$  and HQC, the concentration of free metal ion  $[\text{M}^{n+}]$  for use in Eq. (1) is calculated as half the total metal ion concentration at the  $\text{pK}_a(2)$  (apparent) in equation [3]. This is because at the mid-point of equilibrium [3], where  $\text{pK}_a(2)$  (apparent) is measured,  $[\text{M}^{n+}] = [\text{M}(\text{HQCH})^{+}]$ . For weakly coordinating metal ions ( $\text{Mg(II)}$ ,  $\text{Ca(II)}$ ,  $\text{Sr(II)}$ ,  $\text{Ba(II)}$ ), large excesses of metal ion were present to promote complex formation, and  $[\text{M}^{n+}]$  was calculated as  $M_{\text{total}} - [\text{M}(\text{HQCH})]^{+}$ .

For more acidic metal ions, additional acid–base equilibria occur at higher pH, which are interpreted as deprotonation of waters coordinated to the metal ion (or its stoichiometric equivalent, addition of hydroxide), such as those in Eq. (4):



This interpretation is particularly reasonable because (1) the changes in the spectra in the pH range where these equilibria are postulated to occur are comparatively small, consistent with deprotonation of waters attached to the metal ion, and therefore more remote from the chromophore of the ligand, and (2) the two deprotonation equilibria at lower pH are accompanied by spectral changes that resemble those for other metal ions such as  $\text{Ca(II)}$  or  $\text{Mg(II)}$  that have only the equilibria indicated in 2 and 3, and therefore can be reasonably assumed to correspond to these equilibria. The formation constants determined here are given in Table 6.

### 2.5. Molecular mechanics calculations

These were carried out using the molecular modeling program HyperChem [26], which utilizes an extended version of the program MM2 [27].

## 3. Results and discussion

### 3.1. Structural studies

The structures of **1** and **2** shown in Figs. 2 and 3 are a little surprising in that  $\text{M}(\text{LH})_2$  complexes were obtained in spite of the fact that the syntheses employed 1:1 M:L ratios (LH denotes that the coordinated HQC ligand has a protonated phenolate). One should say at once, of course, that there is no necessary correspondence between solution species and species isolated in the solid state. The presence of  $\text{M}(\text{LH})_2$  complexes possibly reflects the synthetic method employed, where the ligand was dissolved in an organic phase immiscible with the aqueous phase containing the metal ion. The ratio of ligand to metal at the interface of the two solvents might not necessarily be the same as that of the bulk liquids. In particular, one might imagine that once one had formed an ML complex, it would be more organic soluble, and would readily react with a second ligand molecule in the organic phase. The HQC complexes obtained here for  $\text{Zn(II)}$  and  $\text{Cd(II)}$  appear to be isomorphous with each other, and also with the  $\text{Co(II)}$  [17] and  $\text{Ni(II)}$  [16] complexes, so that it might also be that the  $[\text{M}(\text{LH})_2] \cdot 3\text{H}_2\text{O}$  type of structure found here is particularly stable.

The crystal structures reported here and elsewhere [16,17] for complexes of HQC, where the phenolate is protonated, support the observation of complexes in solution where, from the spectrophotometric studies described below, it is considered that protonated MLH complexes are being formed, and indicate that the complexes contain a protonated phenolate group coordinated to the metal ion. The  $\text{Zn(II)/HQC}$  structure (**1**) has distorted octahedral



geometry around the Zn(II), with one Zn–N bond that is rather short at 2.00 Å, while the other is more normal at 2.15 Å. This can be compared with Zn–N bond distances to pyridyl groups that are part of chelate rings in the CSD (288 structures with  $R < 0.1$ , 950 individual chelate rings, six-coordinate Zn), which average  $2.15, \pm 0.06$  Å. It appears to be a general feature of HQC complexes of metal ions that are too small to complex in a low-strain fashion with the ligand, that the M–N bonds are shorter than usual, while the M–O bonds are much longer. This is seen in Table 5 for  $[M(\text{HQCH})_2] \cdot 3 \text{H}_2\text{O}$  complexes where M–L bond lengths for Ni(II), Co(II), Zn(II) and Cd(II) are compared with typical M–L bonds of the same type in the CSD [22]. What one sees in the Zn(II) structure is that one phenolate (O(1)) has a very long Zn–O bond of 2.43 Å, while the other (O(4)) is fairly short at 2.22 Å. The long Zn–O bond has a proton at normal O–H bond distances attached to the phenolic oxygen. In contrast, the short Zn–O bond has its proton displaced from the phenolic oxygen (O(4)) to form a short (O–O = 2.452 Å) symmetrical H-bond with a neighboring water molecule. The possible significance of these H-bonds is discussed below. What is of particular interest in Fig. 2 is that the water molecule H-bonded to the phenolic O(4) atom is held in place by two very short H-bonds (Fig. 2) of (O–O separation) 2.452 and 2.497 Å, in addition to a third somewhat longer H-bond with an O–O distance of 2.626 Å. A search of the CSD reveals no structure involving either waters or alcohols where these are held in place by two very short H-bonds with both O–O separations less than 2.50 Å. The structure of  $[\text{Cd}(\text{HQCH})_2] \cdot 3\text{H}_2\text{O}$  (2) has the longest M–L bonds with HQC as a ligand. The Cd–N bonds average 2.223 Å, while the Cd–O bonds to the phenolate oxygens average 2.37 Å, which is the only one of these HQC complexes where these bonds are not greatly elongated as compared to the examples of less strained M–O bonds involving phenols in the CSD.

What is rather interesting in the structures of HQC complexes is the presence of coordinated HQC ligands that are protonated. All of the protonated phenolate groups are accompanied by water molecules that form very short H-bonds, with O–O distances in the range 2.45–2.56 Å. In addition, one of the two phenolate oxygens forms H-bonds to second water molecules with more normal O–O separations of about 2.8 Å. These H-bonds are summarized in Table 4. Short H-bonds, in the range 2.4–2.5 Å, which are very stable, are currently of considerable interest [18] because of their possible catalytic role in biology. Short H-bonds involving other  $\text{RO}^-$  groups coordinated to metal ions have been reported for complexes of ligands of the type  $\text{THE-9-aneN}_3$  [29–31]. For the Zn(II)/HQC structure, one of the two coordinated phenolic O-donors forms a short (2.559 Å) but otherwise unremarkable H-bond. However, the other phenolate forms a short symmetrical H-bond to a water molecule, as shown in Fig. 6. The Cd(II) takes this one step further (Fig. 6) in that the proton appears to reside on the water molecule adjacent to the phenolate, in the form of a hydronium ion. Of course, one should be a little cautious about assigning positions of H-atoms from crystallographic studies, particularly in the presence of heavy metal atoms such as Cd. However, the more certainly known O–O separations for the Cd(II) compound show a different pattern to those of the other metal ions, supporting the idea that the proton in the Cd(II) complex is in a different situation, and is located on a water molecule as a hydronium ion, rather than being located on the phenolate. In particular, the O–O distance of the H-bond to the second water molecule (Ow(2)) in Fig. 6) is shortest for the Cd(II) complex, as would be expected if this phenolate had lost its proton, and so was more attractive to the adjacent water molecule (Ow(2)). One thus has an intriguing series, where for the Co(II) and Ni(II) complexes the proton is located (Fig. 6) on the phenolate oxygen, with a longer bond to the H-bonded

Table 4

Hydrogen-bonding O–O distances involving the coordinated phenol groups of HQC complexes in the  $[M(\text{HQCH})_2] \cdot 3\text{H}_2\text{O}$  complexes<sup>a</sup>

Metal ion	O...O H-bond distance (Å)	Nature of H-bonds <sup>b</sup>	Reference
Ni(II)	2.465 <sup>c</sup>	<u>PhOH</u> ... <u>OH</u> <sub>2</sub> (asymmetrical, O–H of PhOH = 0.81 Å)	[15]
	2.889 <sup>c</sup>	<u>PhHO</u> ... <u>HOH</u>	[15]
	2.555	<u>PhOH</u> ... <u>OH</u> <sub>2</sub>	[15]
Co(II)	2.459 <sup>c</sup>	<u>PhOH</u> ... <u>OH</u> <sub>2</sub> (asymmetrical, O–H of PhOH = 0.92 Å)	[16]
	2.896 <sup>c</sup>	<u>PhHO</u> ... <u>HOH</u>	[16]
	2.565	<u>PhOH</u> ... <u>OH</u> <sub>2</sub>	[16]
Zn(II)	2.452 <sup>c</sup>	<u>PhO</u> – <u>H</u> – <u>OH</u> <sub>2</sub> (symmetrical, O–H = 1.214, 1.216 Å)	this work
	2.784 <sup>c</sup>	<u>PhHO</u> ... <u>HOH</u>	this work
	2.559	<u>PhOH</u> ... <u>OH</u> <sub>2</sub>	this work
Cd(II)	2.496 <sup>c</sup>	<u>PhO</u> <sup>−</sup> ... <u>HOH</u> <sub>2</sub> <sup>+</sup> (hydronium ion)	this work
	2.768 <sup>c</sup>	<u>PhO</u> <sup>−</sup> ... <u>HOH</u> (water molecule)	this work
	2.568	<u>PhOH</u> ... <u>OH</u> <sub>2</sub> (water molecule)	this work

<sup>a</sup> Abbreviation: PhO = phenolic group coordinated to metal ion.

<sup>b</sup> The atoms involved in forming the H-bond are underlined.

<sup>c</sup> For each metal ion complex, these two H-bonds involve the same phenolic oxygen.

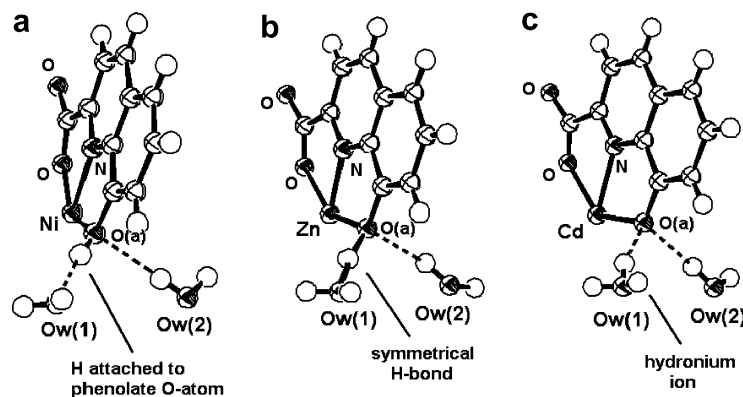


Fig. 6. Hydrogen-bonded phenolate oxygens (O(a)) in the structures of Ni(II) [15], Zn(II) (this work), and Cd(II) (this work) complexes of HQC. For clarity, only the HQC ligand involved in the structurally varying H-bonds on each complex is shown. The O–O distances from the coordinated phenolate oxygens (O(a)) to the H-bonded H<sub>2</sub>O molecules Ow(1) are all very short at 2.465 (Ni), 2.452 (Zn), and 2.496 Å (Cd). The metal to O(a) distances are such that Ni–O is longer than normal (see text) by 0.23 Å, Zn–O by 0.10 Å, and Cd–O by only 0.03 Å. Accompanying this the O–O distances to the second H-bonded water molecule (Ow(2)) decrease as 2.889 (Ni), 2.784 (Zn) and 2.768 Å (Cd). Drawing made using ORTEP [28].

water. For the Zn(II) complex the H-bond appears to be symmetrical, and finally, for the Cd(II) complex the proton is located on the water molecule as a hydronium ion. The metal ions thus appear to tune the basicity of the phenolate O-donor to which they are coordinated. This presumably arises because the Ni–O bond length to the phenolate O-donor is very long for a Ni–O bond at 2.227 Å, the Zn–O bond is more normal at 2.22 Å, while the Cd–O bond length is near-normal at 2.334 Å. The extent of normality of these M–O bonds can be judged from structures in the CSD, as seen in Table 5. Thus, one can see that the rigid structure of the HQC ligand has stretched the Ni–O bond by some 0.23 Å, while at the other extreme the Cd–O bonds in the HQC complexes are stretched by 0.06 Å. The Zn/HQC complex actually provides two very different Zn–O lengths. For the short Zn–O (phenolate) bond, the proton is removed to form a symmetrical H-bond, whereas for the long Zn–O, the proton is found at a normal O–H distance. One can thus reasonably suggest that as the contact between the metal ion and the phenolate oxygen is stretched away from normal, so the basicity of the phenolate increases and the proton is more strongly bound to it. In the case of the Cd(II) complex, the contact between the metal ion and the phenolate is very strong, and the proton

is attached to the water molecule as a hydronium ion. In spite of the possible uncertainty of placing the proton as a hydronium ion in the presence of the heavy Cd atom, the O–O distances to the second water molecule H-bonded to this phenolate oxygen support the idea that the proton in the Cd(II) complex is not attached to the phenolate oxygen. Thus, this H-bond is shorter in the Cd(II) complex (2.768 Å) than in the Zn(II) (2.784 Å) or Ni(II) complex (2.889 Å), in line with what would be expected if the interaction of the proton with this phenolate oxygen decreased Ni(II) > Zn(II) > Cd(II).

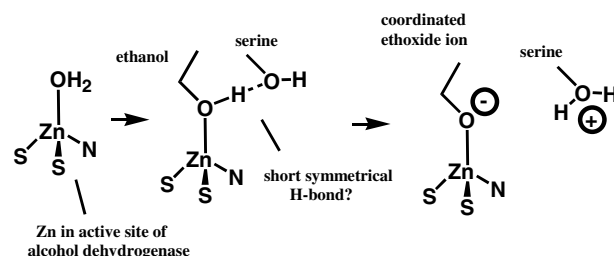
One can tentatively suggest that the above series gives one an idea of how the proton transfer in alcohol dehydrogenase (ADH) from the alcohol in the ADH binding site to an adjacent serine, as promoted by coordination of the alcoholic oxygen to the Zn(II) in ADH, might appear [20]. The Zn(II) ion in alcohol dehydrogenase (ADH) binds to the oxygen of the alcoholic substrate and initiates a chain of proton transfers that results in the deprotonation of the alcoholic hydroxyl group. It is thought [20] that this process involves the formation of a short symmetrical low-energy H-bond as suggested in Scheme 1.

The formation of the ethoxide ion is the step that activates the ethanol, or other alcohol, to oxidation to the aldehyde by transfer of an  $\alpha$ -methylene proton to NAD<sup>+</sup> (nicotinamide adenine dinucleotide). Thus the alcoholic hydroxyl, as in the Ni(II) complex in Fig. 6a, is at a much

Table 5  
M–L bonds lengths in [M(HQCH)<sub>2</sub>]·3H<sub>2</sub>O complexes compared to similar bonds for these metal ions in the CSD [22]

Metal ion	Ni(II)	Co(II)	Zn(II)	Cd(II)
<i>Mean bond lengths (Å)</i>				
M–N in HQC complex	1.976	1.972	2.090	2.223
M–N to pyridyls (CSD)	2.07(6)	2.14(11)	2.15(6)	2.37(6)
M–O (phenol) (HQC)	2.259	2.256	2.22 <sup>a</sup>	2.33 <sup>a</sup>
Mean M–O phenol (CSD)	2.03(6)	2.03(5)	2.07(6)	2.27(1)

<sup>a</sup> These are the bonds to the phenolate (Zn–O(3) and Cd–O(3)) where in the Zn(II) complex a short symmetrical H-bond is formed to an adjacent water molecule, and in the Cd(II) complex the proton is removed from the phenolate to form a hydronium ion on an adjacent water molecule. Ni(II) and Co(II) structures from Refs. [15,16].



Scheme 1.

longer distance than the bonding distance from the metal ion. In this situation, the proton is attached to the phenolic oxygen, resembling the alcohol with its proton still attached to the alcoholic oxygen. In the Zn(II) structure in Fig. 6b, which is now closer to a normal M–O length, the proton is beginning to move away from the phenolate oxygen, and a symmetric H-bond with the adjacent water is formed. Finally, in Fig. 6c, the Cd(II) complex, the metal approaches the phenolate oxygen to within a near-normal M–O bond length, and the proton is completely transferred to the adjacent H-bonded water. In this it resembles the proposed [20] final transfer of the proton to an adjacent serine in the binding site of ADH. One should point out that the Zn(II) in ADH is four-coordinate, and so the comparison here suffers from the fact that the Zn(II) in its HQC complex here might be regarded as five or possibly six-coordinate.

#### 4. Formation constant studies

The HQC system is ideal for study by means of electronic spectroscopy. The intense bands in the range 200–350 nm allow for study of the ligand/metal ion systems at low concentrations of  $2 \times 10^{-5}$  M. The spectra vary strongly as a function of pH, and indicate two protonation constants in the pH range 2–12. The variation of the spectra of  $2 \times 10^{-5}$  M HQC as a function of pH is shown in Fig. 4. The protonation that occurs at pH 9.98 can reasonably be ascribed to protonation of the phenolate oxygen, by comparison with  $pK_a(1)$  of oxine of 9.65[12]. Use of the SOLVER data-fitting module of EXCEL [25] shows that a model involving two protonations satisfactorily accounts for the spectral changes in the pH range 2–12 studied. The second protonation constant presumably involves attachment of the proton to the pyridine nitrogen, as supported by the crystal structure of the diprotonated HQC ligand [16], where one proton is attached to the phenolate oxygen and one to the N-donor. These results suggest that protonation of the carboxylate occurs below pH 2, which is reasonable in comparing the protonation constants [12] of HQC with those of picolinic acid, where  $pK_a(2)$  is only [12] 0.95.

The  $\log K_1$  values for HQC are shown in Table 6. Use of the UV spectra in the range 200–300 nm to monitor the formation of HQC complexes appears to be successful. Weakly binding metal ions such as Mg(II), Ca(II), Sr(II), and Ba(II) show inflections in their spectra as a function of pH that resemble those for the HQC ligand alone, but with the two protonations displaced to lower pH, from which displacements  $\log K_1$  can be calculated. More strongly binding metal ions show similar sets of spectra, but with additional protonations apparent at higher pH values. These are reasonably ascribed to the deprotonation of water molecules attached to the metal ions.

The  $\log K_1$  (HQC) values determined here are compared in Table 7 with  $\log K_1$  values [12] for the ligands oxine, PIC, and DIPIC. As can be seen from Fig. 1, HQC is related to

Table 6

Protonation and formation constants for HQC (8-hydroxyquinoline-2-carboxylic acid = L) reported here<sup>a</sup>

Equilibrium	Log <i>K</i>	No. of points <sup>b</sup>	Reference
$H^+ + OH^- \rightleftharpoons H_2O$	13.78		[12]
$L^{2-} + H^+ \rightleftharpoons LH^-$	9.98(2)	80	this work
$LH^- + H^+ \rightleftharpoons LH_2$	3.94(2)		this work
$Mg^{2+} + L^{2-} \rightleftharpoons MgL$	4.12(5)	90	this work
$MgL + H^+ \rightleftharpoons MgLH^+$	7.53(5)		this work
$Ca^{2+} + L^{2-} \rightleftharpoons CaL$	6.00(5)	105	this work
$CaL + H^+ \rightleftharpoons CaLH^+$	7.11(2)		this work
$Sr^{2+} + L^{2-} \rightleftharpoons SrL$	4.45(5)	100	this work
$SrL + H^+ \rightleftharpoons SrLH^+$	7.70(3)		this work
$Ba^{2+} + L^{2-} \rightleftharpoons BaL$	3.93(7)	95	this work
$BaL + H^+ \rightleftharpoons BaLH^+$	8.10(6)		this work
$La^{3+} + L^{2-} \rightleftharpoons LaL^+$	11.26(5)	95	this work
$LaL^+ + H^+ \rightleftharpoons LaLH^{2+}$	4.40(5)		this work
$LaLOH + H^+ \rightleftharpoons LaL^+$	8.67(5)		this work
$Gd^{3+} + L^{2-} \rightleftharpoons GdL^+$	12.16(5)	95	this work
$GdL^+ + H^+ \rightleftharpoons GdLH^{2+}$	3.87(5)		this work
$GdLOH + H^+ \rightleftharpoons GdL$	9.49(4)		this work
$Cd^{2+} + L^{2-} \rightleftharpoons CdL$	8.57(5)	95	this work
$CdL + H^+ \rightleftharpoons CdLH^+$	6.64(6)		this work
$CdLOH^- + H^+ \rightleftharpoons CdL$	9.29(5)		this work
$Ni^{2+} + L^{2-} \rightleftharpoons NiL$	10.86(5)	110	this work
$NiL + H^+ \rightleftharpoons NiLH^+$	5.64(5)		this work
$NiLOH^- + H^+ \rightleftharpoons NiL$	9.22(5)		this work
$CuL + H^+ \rightleftharpoons CuLH^+$	6.29(6)	90	this work
$CuLOH^- + H^+ \rightleftharpoons CuL$	10.15(4)		this work
$Pb^{2+} + L^{2-} \rightleftharpoons PbL$	12.92(5)	90	this work
$PbL + H^+ \rightleftharpoons PbLH^+$	3.49(5)		this work
$Zn^{2+} + L^{2-} \rightleftharpoons ZnL$	9.10(5)	95	this work
$ZnL + H^+ \rightleftharpoons ZnLH^+$	6.13(5)		this work
$ZnLOH^- + H^+ \rightleftharpoons ZnL$	8.63(5)		this work
$ZnL(OH)_2 + H^+ \rightleftharpoons ZnLOH^-$	11.35(5)		this work

<sup>a</sup> In 0.1 M NaClO<sub>4</sub> at 25.0 °C. Standard deviations are those given by the Solvstat macro provided with Ref. [25].

<sup>b</sup> The numbers of points used in the calculations on each titration are given. Absorbances were measured at five different wavelengths for each titration, so that each pH for which absorbances were measured yielded five separate data points.

oxine by addition of a carboxylate to its two position, while DIPIC is structurally similar to HQC except that a phenolate group in HQC is replaced by a carboxylate in DIPIC. PIC is DIPIC with one less carboxylate, and so is an analog of oxine. What one sees for the small low-acidity Mg(II) ion is that for the HQC complex compared to the oxine complex, the extra carboxylate group of HQC has produced no stabilization relative to oxine. One would surmise that the small Mg(II) ion ( $R^+ = 0.74 \text{ \AA}$  [13]) is unable to bond simultaneously to the acetate and the phenolic oxygen of HQC. A similar effect is seen in comparing PIC and DIPIC in Table 7. For the small Zn(II) and Ni(II) ions, there is likewise little increase in  $\log K_1$  in passing from the oxine to the HQC complexes or the PIC to the DIPIC complexes. In contrast, for the large Group 2 metal ions Ca(II), Sr(II), and Ba(II), there are substantial increases in  $\log K_1$  in comparing HQC and oxine, or DIPIC and PIC complexes. For the large, more acidic, La(III) and Gd(III) ions, the increases in  $\log K_1$  in passing from oxine to HQC, or PIC to DIPIC are very large, as would be expected



Table 7

Comparison of  $\log K_1$  values for HQC determined here with those [12] for oxine, DIPIC, and PIC<sup>a</sup>

Metal ion	Mg(II)	Ca(II)	Sr(II)	Ba(II)	La(III)	Gd(III)	Cd(II)	Ni(II)	Zn(II)	Pb(II)	Cu(II)
Ionic radius (Å) <sup>b</sup>	0.74	1.00	1.18	1.36	1.03	0.94	0.95	0.69	0.74	1.19	0.57
$\log K_1$ (OH <sup>−</sup> ) <sup>c</sup>	2.58	1.30	0.82	0.64	5.5	6.3	3.9	4.1	5.0	6.4	6.5
$\log K_1$ (HQC)	4.12	6.00	4.45	3.93	11.26	12.16	8.57	10.86	9.10	12.92	13.2
$\log K_1$ (oxine)	4.31	2.82	2.11	1.62	5.9	7.0	7.34	9.27	8.52	9.02	12.0
$\log K_1$ (dipic)	2.34	4.36	3.85	3.44	7.94	8.69	6.36	6.95	6.35	8.70	9.10
$\log K_1$ (pic)	2.21	1.80	1.69	1.65	3.51	3.98	4.35	6.72	5.23	4.58	7.87

<sup>a</sup> All at ionic strength 0.1, 25 °C.<sup>b</sup> Ref. [13] for six-coordination, except Cu(II) = square planar.<sup>c</sup> From Ref. [12], ionic strength = 0.

(Increasing metal ion acidity is indicated in Table 7 by increasing  $\log K_1$  (OH<sup>−</sup>) values [12].).

#### 4.1. MM calculations

One can carry out MM calculations of the strain energy for complexes of the type  $[M(HQC)(H_2O)_3]$  as a function of ideal bond length to determine the best-fit size of metal ion for coordinating to the HQC ligand [32,33]. In these calculations all of the force-constants were kept at the default values in the HyperChem program [26] for high-spin Ni(II), while the ideal M–N bond length was varied over the range 1.8–3.2 Å, and the accompanying values of the ideal M–O bond length were kept a constant 0.06 Å shorter than the M–N length. The constant difference in M–N and M–O bond length arises because the ionic radius [13] of the O-donor is 0.06 Å less than that of the N-donor. Such a curve (Fig. 7) for  $U_{ML}$  versus M–N length has a minimum at M–N = 2.52 Å, which is typical for

ligands forming complexes that contain only five-membered chelate rings. With an ionic radius [13] for the N-donor of 1.46 Å, this means that metal ions with an ionic radius [13] ( $r^+$ ) of about 1.06 Å should coordinate with HQC with least steric strain. This agrees well with the  $\log K_1$  values for HQC in Table 1. Thus, larger metal ions such as Ca(II) ( $r^+ = 1.00$  Å), La(III) ( $r^+ = 1.03$  Å) and Pb(II) ( $r^+ = 1.19$  Å) show the largest increases in  $\log K_1$  in passing from oxine to HQC. There is also a contribution to this from metal ion acidity, so that large acidic metal ions such as La(III) show the greatest increases.

#### 5. Conclusions

The study here shows the strong metal ion complexing ability of the ligand HQC, which is highly preorganized by its rigid aromatic backbone. The presence of five-membered chelate rings as formed by HQC on complex-formation particularly favors complex-formation with large metal ions, and the high basicity of the phenolate group on HQC means that complex stability is particularly high with large more acidic metal ions such as La(III) or Gd(III). The approach to preorganization embodied in HQC suggests that other highly preorganized ligands based on rigid aromatic backbones should have useful and interesting metal ion coordinating properties. In this, HQC resembles the highly preorganized ligand PDA (1,10-phenanthroline-2,9-diacetate) which shows [34] strong preference for metal ions such as Cd(II) or Gd(III) that have ionic radii in the vicinity of 1.0 Å, and complexes of very high thermodynamic stability. The structures of the  $[M(HQCH)_2] \cdot 3H_2O$  complexes (M = Co(II), Ni(II), Zn(II), and Cd(II)) all show very short (<2.50 Å) O–O separations in the H-bonds formed between protonated phenolates coordinated to the metal ions, and adjacent water molecules, which may be of interest in light of suggestions [18–20] about the role of low-barrier H-bonds in the functioning of enzymes such as ADH (alcohol dehydrogenase). These structures provide an interesting sequence where the proton on one coordinated phenol initially resides on the phenolic oxygen when the small metal (Co(II), Ni(II)) ions have very long M–O bonds to that oxygen, but as the M–O bond approaches more normal bond lengths, it first forms a short symmetrical H-bond (Zn(II)), and then with the

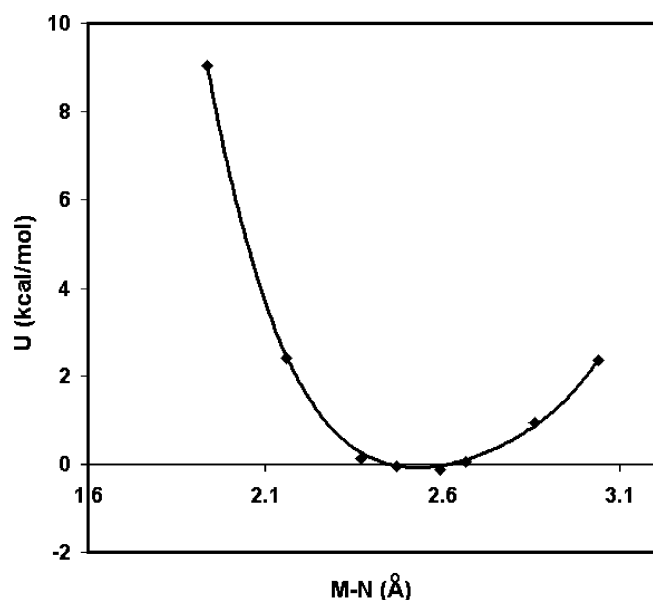


Fig. 7. Variation of strain energy ( $U$ ) for complexes of the type  $[M(HQC)(H_2O)_3]$  as a function of ideal M–N length, calculated as described in the text. The curve shows that the best-fit size metal ion will have a M–N length of 2.52 Å.

large Cd(II) ion, where more effective contact is made with this oxygen, the proton is transferred to an adjacent water molecule.

### Acknowledgements

The authors thank the University of North Carolina Wilmington and the National Science Foundation (Grant # CHE0111131) for generous support of this work.

### Appendix A. Supplementary material

Supplementary data associated with this article can be found, in the online version, at [doi:10.1016/j.ica.2007.10.004](https://doi.org/10.1016/j.ica.2007.10.004).

### References

- [1] D.W. Cram, *Science* 240 (1988) 76.
- [2] R.D. Hancock, A.E. Martell, *Chem. Rev.* 89 (1989) 1875.
- [3] See C. Orvig, M. Abrams, *Chem. Rev.* 99 (1999) 2201, and the following papers in that issue.
- [4] L.R. Morss, M.A. Lewis, M.K. Richmann, D. Lexa, *J. Alloys Compd.* 42–48 (2000) 303.
- [5] C.J. Pedersen, *Angew. Chem.* 100 (1988) 1053.
- [6] T.J. Hubin, J.M. McCormick, N.W. Alcock, D.H. Busch, *Inorg. Chem.* 40 (2001) 435.
- [7] C.J. Pederson, J.M. Lehn, D.J. Cram, *Resonance* 6 (2001) 71.
- [8] A.S. De Sousa, G.J.B. Croft, C.A. Wagner, J.P. Michael, R.D. Hancock, *Inorg. Chem.* 30 (1991) 3525.
- [9] A.S. De Sousa, R.D. Hancock, J.H. Reibenspies, *J. Chem. Soc., Dalton Trans.* (1997) 939.
- [10] A.S. De Sousa, R.D. Hancock, J.H. Reibenspies, *J. Chem. Soc., Dalton Trans.* (1997) 2831.
- [11] R.D. Hancock, A.S. de Sousa, G.B. Walton, J.H. Reibenspies, *Inorg. Chem.* 46 (2007) 4749.
- [12] A.E. Martell, R.M. Smith, *Critical Stability Constant Database*, 46, National Institute of Science and Technology (NIST), Gaithersburg, MD, USA, 2003.
- [13] R.D. Shannon, *Acta Crystallogr., Sect. A* 32 (1976) 751.
- [14] T. Hata, T. Uno, *Bull. Chem. Soc. Jpn.* 45 (1972) 2497.
- [15] M. Nakamura, C. Kitamura, H. Ueyama, K. Yamana, A. Yoneda, *Cryst. Struct. Rep.* 21 (2005) x115.
- [16] N. Okabe, Y. Muranishi, *Acta Crystallogr., Sect. C* 58 (2002) m475.
- [17] N. Okabe, Y. Muranishi, *Acta Crystallogr., Sect. E* 58 (2002) m352.
- [18] J.A. Gerit, M.M. Kreevoy, W.W. Cleland, P.A. Frey, *Chem. Biol.* 4 (1997) 259.
- [19] T. Steiner, W. Saenger, *Acta Crystallogr., Sect. B* 50 (1994) 348.
- [20] L.A. LeBrun, D.-H. Park, S. Ramaswamy, B.V. Plapp, *Biochemistry* 43 (2004) 3014.
- [21] E.J. Gabe, Y. Le Page, J.-P. Charland, F.L. Lee, P.S. White, *J. Appl. Cryst.* 22 (1989) 384.
- [22] C.H. Gorbitz, *Acta Crystallogr., Sect. B* 55 (1999) 1090.
- [23] Cambridge Crystallographic Data Centre, 12 Union Road, Cambridge CB2 1EZ, United Kingdom.
- [24] Y.X. Xia, G.R. Choppin, *Talanta* 43 (1996) 2073.
- [25] E.J. Billo, *EXCEL for Chemists*, Wiley-VCH, New York, 2001.
- [26] Hyperchem program, version 7.5, Hypercube, Inc., 419 Philip Street, Waterloo, Ontario, N2L 3X2, Canada.
- [27] N.L. Allinger, *J. Amer. Chem. Soc.* 98 (1977) 8127.
- [28] ORTEP-3 for Windows, Version 1.08, L.J. Farrugia, *J. Appl. Cryst.* 30 (1997) 565.
- [29] A.A. Belal, L.J. Farrugia, R.D. Peacock, J. Robb, *J. Chem. Soc., Dalton Trans.* (1989) 931.
- [30] R. Luckay, R.D. Hancock, I. Cukrowski, J.H. Reibenspies, *Inorg. Chim. Acta* 246 (1996) 159.
- [31] L.J. Farrugia, N.N. MacDonald, R.D. Peacock, J. Robb, *Polyhedron* 14 (1995) 541.
- [32] R.D. Hancock, *Acc. Chem. Res.* 23 (1990) 253.
- [33] R.D. Hancock, *Progr. Inorg. Chem.* 36 (1989) 187.
- [34] D.L. Melton, D.G. VanDerveer, R.D. Hancock, *Inorg. Chem.* 45 (2006) 9306.